



**HAL**  
open science

## Goniopolarimetric inversion using SVD: An application to type III radio bursts observed by STEREO

V. Krupar, O. Santolik, B. Cecconi, M. Maksimovic, X. Bonnin, M. Panchenko, A. Zaslavsky

### ► To cite this version:

V. Krupar, O. Santolik, B. Cecconi, M. Maksimovic, X. Bonnin, et al.. Goniopolarimetric inversion using SVD: An application to type III radio bursts observed by STEREO. *Journal of Geophysical Research Space Physics*, 2012, 117 (A6), pp.n/a-n/a. 10.1029/2011JA017333 . hal-02881485

**HAL Id: hal-02881485**

**<https://hal.science/hal-02881485>**

Submitted on 4 Nov 2021

**HAL** is a multi-disciplinary open access archive for the deposit and dissemination of scientific research documents, whether they are published or not. The documents may come from teaching and research institutions in France or abroad, or from public or private research centers.

L'archive ouverte pluridisciplinaire **HAL**, est destinée au dépôt et à la diffusion de documents scientifiques de niveau recherche, publiés ou non, émanant des établissements d'enseignement et de recherche français ou étrangers, des laboratoires publics ou privés.

Copyright

## Goniopolarimetric inversion using SVD: An application to type III radio bursts observed by STEREO

V. Krupar,<sup>1,2,3</sup> O. Santolik,<sup>2,3</sup> B. Cecconi,<sup>1</sup> M. Maksimovic,<sup>1</sup> X. Bonnin,<sup>1</sup> M. Panchenko,<sup>4</sup> and A. Zaslavsky<sup>1</sup>

Received 4 November 2011; revised 27 March 2012; accepted 2 April 2012; published 5 June 2012.

[1] Type III radio bursts are intense solar radio emissions generated by beams of energetic electrons injected into the interplanetary medium. They can be routinely observed by the S/Waves instruments on-board the STEREO (Solar Terrestrial Relation Observatory) spacecraft. We describe goniopolarimetric (GP) inversion of a signal measured on non-orthogonal antennas using the Singular Value Decomposition (SVD) technique. This wave propagation analysis can be applied to spectral matrices built from measurements by the High Frequency Receiver (HFR; a part of the S/Waves experiment). We have found an empirical relation between the decomposed spectral matrices and apparent source sizes for waves with a low degree of polarization. Simulations of electromagnetic emissions with various senses and degrees of polarization, and source shapes show that SVD gives us reasonable results with respect to the polarization ellipsoid geometry. An error analysis considering inaccuracies of HFR has been performed in order to test the validity of the  $\mathbf{k}$ -vector direction estimation and the obtained empirical relation. We present a joint observation of a type III radio burst by the STEREO and *Wind* spacecraft during small separation distances. We obtain consistent results for the  $\mathbf{k}$ -vector direction and apparent source size using different analysis methods for the measurements of the STEREO and *Wind* spacecraft. We demonstrate that SVD can be an effective tool for the wave analysis of radio emissions measured on non-orthogonal antennas even with very extended sources.

**Citation:** Krupar, V., O. Santolik, B. Cecconi, M. Maksimovic, X. Bonnin, M. Panchenko, and A. Zaslavsky (2012), Goniopolarimetric inversion using SVD: An application to type III radio bursts observed by STEREO, *J. Geophys. Res.*, *117*, A06101, doi:10.1029/2011JA017333.

### 1. Introduction

[2] Type III radio bursts are among the most intense electromagnetic emissions in the heliosphere [Wild, 1950]. They are generated by beams of suprathermal electrons ( $\sim 0.1c$ ) accelerated near the Sun's surface and streaming outward along the open magnetic field lines and connected with solar flares and/or coronal mass ejections (CMEs) driven shocks. The electron beams, when they pass through the medium along the Parker spiral magnetic field lines, produce locally a bump-on-tail instability in the local

electron distribution function. This change of plasma parameters can lead to generation of electrostatic Langmuir waves at the local plasma frequency  $f_p$ , which can be afterwards converted by a nonlinear conversion into electromagnetic waves: type III radio bursts. This conversion involves interaction with low frequency plasma waves and/or scattering at ion density fluctuations resulting in radio bursts at  $f_p$  (fundamental emission) and/or  $2f_p$  (harmonic emission) beamed tangent to the Parker spiral. Although a basis of this conversion has been formulated by Ginzburg and Zhelezniakov [1958], the whole process is still not well understood and several theories remain under debate, e.g., stochastic-growth theory (SGT) [Cairns and Robinson, 1995]. As electron beams propagate outward from the Sun, these emissions are generated at lower frequencies corresponding to a decreasing of  $f_p$  which is related to the local plasma density:  $f_p$  (kHz)  $\approx 9\sqrt{n(\text{cm}^{-3})}$ . Type III radio bursts display maximal flux density approximately at 1 MHz [Weber, 1978]. In comparison with other electromagnetic emissions, their sources are apparently extended [Steinberg et al., 1984, 1985; Bonnin et al., 2008], which can be explained by either properties of an intrinsic beaming pattern and/or scattering by density fluctuations of the interplanetary medium. Hence an estimation of their apparent

<sup>1</sup>Laboratoire d'Etudes Spatiales et d'Instrumentation en Astrophysique, UMR CNRS 8109, Observatoire de Paris, Meudon, France.

<sup>2</sup>Faculty of Mathematics and Physics, Charles University, Prague, Czech Republic.

<sup>3</sup>Institute of Atmospheric Physics, Czech Academy of Science, Prague, Czech Republic.

<sup>4</sup>Space Research Institute, Austrian Academy of Sciences, Graz, Austria.

Corresponding author: V. Krupar, Laboratoire d'Etudes Spatiales et d'Instrumentation en Astrophysique, UMR CNRS 8109, Observatoire de Paris, 5, Place Jules Janssen, F-92195 Meudon CEDEX, France. (vratislav.krupar@obspm.fr)

source size could yield important information about density fluctuations in the solar wind. Although coronal type III radio bursts ( $f \sim 200$  MHz) can have up to 35% of the circular polarization, the degree of polarization of type III radio bursts at long wavelengths ( $f \sim 1$  MHz) is negligible [Dulk, 2000]. Multipoint observations of type III radio bursts using goniopolarimetric (GP, also referred to as direction-finding) products have already been obtained by spinning spacecraft [Gurnett et al., 1978; Manning and Fainberg, 1980; Hoang et al., 1981]. This paper presents general GP methods for three axis stabilized spacecraft.

[3] For determining the wave vector ( $\mathbf{k}$ ) directions and polarization parameters we need instruments allowing multicomponent measurements of auto-correlations and cross-correlations of the voltages induced by the wave electric and/or magnetic field. These instruments provide us with the GP data, which can be used for advanced analysis of an incoming wave [Lecacheux, 1978; Ladreiter et al., 1995; Cecconi et al., 2008]. With such data we are able to compose an orthogonal spectral matrix  $S_{ij}$  containing the information about the incident wave:

$$S_{ij} = \langle E_i E_j^* \rangle, \quad (1)$$

where  $E_k$  is a vector of complex amplitudes, indices  $i$  and  $j$  represent three Cartesian components,  $\langle \rangle$  means time averaging on a time interval much longer than the observed wave period and  $*$  corresponds to a complex conjugate. The Singular Value Decomposition (SVD) is an efficient tool for wave analysis [Santolík et al., 2003] that can be directly utilized on a  $6 \times 3$  matrix  $\mathbf{A}$  containing separated real and imaginary parts of a  $3 \times 3$  complex spectral matrix  $S_{ij}$ :

$$\mathbf{A} = \begin{pmatrix} S_{11} & \text{Re}(S_{12}) & \text{Re}(S_{13}) \\ \text{Re}(S_{12}) & S_{22} & \text{Re}(S_{23}) \\ \text{Re}(S_{13}) & \text{Re}(S_{23}) & S_{33} \\ 0 & -\text{Im}(S_{12}) & -\text{Im}(S_{13}) \\ \text{Im}(S_{12}) & 0 & -\text{Im}(S_{23}) \\ \text{Im}(S_{13}) & \text{Im}(S_{23}) & 0 \end{pmatrix}. \quad (2)$$

Applying SVD on this special real form of the complex spectral matrix we obtain real matrices  $\mathbf{U}$ ,  $\mathbf{W}$  and  $\mathbf{V}^T$ :

$$\mathbf{A} = \mathbf{U} \cdot \mathbf{W} \cdot \mathbf{V}^T. \quad (3)$$

The SVD inversion retrieves information about the axis directions/lengths of the polarization ellipsoid (the wave vector direction/ellipticity) and estimators of the planarity of polarization. The  $\mathbf{U}$  matrix is a  $6 \times 3$  matrix with orthonormal columns used in the decomposition of  $\mathbf{A}$ . Polarization properties and estimation of an angular source size are defined by the matrix  $\mathbf{W}$ , which is a diagonal matrix  $3 \times 3$  of three positive or null singular values that represent the axis lengths of the polarization ellipsoid. The  $3 \times 3$  matrix  $\mathbf{V}^T$  with orthonormal rows contains directions of the axes of the polarization ellipsoid. This method was originally designed for  $3 \times 3$  magnetic spectral matrices by assuming that  $\mathbf{B} \cdot \mathbf{k} = 0$  [Santolík et al., 2003]. It can also be used for electric spectral matrices if the condition  $\mathbf{E} \cdot \mathbf{k} = 0$  is fulfilled, which is the case of radio waves when observed far from their propagation mode cutoff.

[4] The influence of extended sources on the measured spectral matrix, which are typical for type III radio bursts at long wavelengths, has been efficiently described by Cecconi [2007] in equations (4)–(10):

$$P_{ij} = \frac{Z_0 G h_i h_j S_0}{2} \left[ (1 + Q) \left( A_i A_j \frac{\Gamma_2}{2} + C_i C_j \left( \Gamma_1 - \frac{\Gamma_2}{2} \right) \right) + (U - iV) \left( A_i B_j \frac{\Gamma_2}{2} \right) + (U + iV) \left( A_j B_i \frac{\Gamma_2}{2} \right) + (1 - Q) \left( A_i A_j \frac{1}{2} \left( \Gamma_1 - \Gamma_2 + \frac{\Gamma_3 + \Gamma_1}{4} \right) + B_i B_j \frac{1}{2} \left( \Gamma_1 + \frac{\Gamma_3 + \Gamma_1}{4} \right) + C_i C_j \left( \frac{\Gamma_2}{2} - \frac{\Gamma_3 + \Gamma_1}{4} \right) \right) \right], \quad (4)$$

$$A_k = -\sin \theta_k \cos \theta \cos(\phi - \phi_k) + \cos \theta_k \sin \theta, \quad (5)$$

$$B_k = -\sin \theta_k \sin(\phi - \phi_k), \quad (6)$$

$$C_k = \sin \theta_k \sin \theta \cos(\phi - \phi_k) + \cos \theta_k \cos \theta, \quad (7)$$

$$\Gamma_k^a(\gamma) = \frac{1}{1 - \cos \gamma} \int_0^\gamma \sin(k\theta'_M) d\theta'_M = \frac{1 - \cos(k\gamma)}{k(1 - \cos \gamma)}, \quad (8)$$

$$\Gamma_k^b(\gamma) = \frac{3}{2} \frac{1}{1 - \cos \gamma} \int_0^\gamma \left( 1 - \frac{\tan^2 \theta'_M}{\tan^2 \gamma} \right)^{1/2} \cdot \sin(k\theta'_M) d\theta'_M, \quad (9)$$

$$\Gamma_k^c(\gamma) = \frac{\ln 2}{1 - \cos \gamma} \int_0^{\pi/2} \exp\left(-\ln(2) \frac{\tan^2 \theta'_M}{\tan^2 \gamma}\right) \cdot \sin(k\theta'_M) d\theta'_M. \quad (10)$$

[5] The  $P_{ij}$  matrix on the left hand side of equation (4) represents a modeled spectral matrix that we will compare with the matrix measured by the instrument.  $P_{ij}$  is generally a non-orthogonal matrix unlike  $S_{ij}$  defined in equation (1). The right hand side of equation (4) contains the impedance of free space ( $Z_0$ ); parameters of the electrical antennas: effective lengths ( $h_k$ ), directions ( $\theta_k$  and  $\phi_k$ ) and gain ( $G$ ); and incident wave properties: the  $\mathbf{k}$ -vector directions ( $\theta$  and  $\phi$ ), the Stokes parameters (the energy flux:  $S_0$ ; the linear polarization degrees:  $Q$  and  $U$ ; and the circular polarization degree:  $V$ ) [Kraus, 1966] and the angular half aperture of the source ( $\gamma$ ), as seen by a spacecraft and contained in the  $\Gamma_k$  coefficients. The shape of the source (see Figure 1), that reflects a radial cut of a source brightness distribution, is considered to be either uniform (equation (8): model 1a), spherical (equation (9): model 1b) or Gaussian (equation (10): model 1c).

[6] In this paper we present results of a GP inversion using the SVD technique considering extended sources of solar radio emissions. In section 2 we describe an empirical relationship between a decomposed spectral matrix and the apparent source size in more detail regarding features of type III radio bursts at long wavelengths. An extensive application of SVD to simulated data with various properties of a source is shown in section 3. Section 4 contains an application of SVD on a single type III radio burst observed by

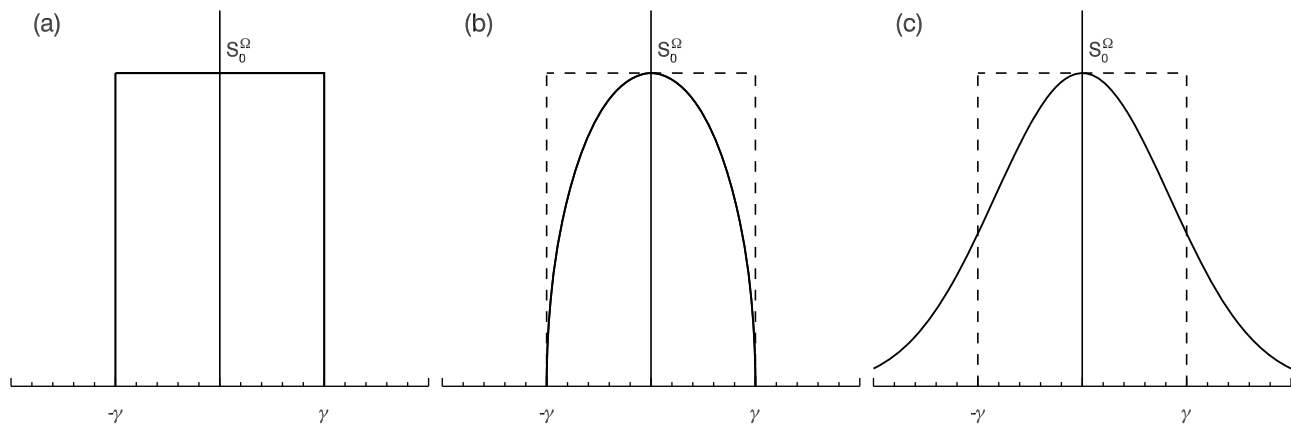


**Figure 1.** Radial cuts of three source brightness distributions: (a) uniform source, (b) spherical source, and (c) Gaussian source (adapted from *Cecconi* [2007]).

the Solar Terrestrial Relation Observatory (STEREO) and *Wind* spacecraft during small separation distances. We show that results obtained from *Wind* using different techniques (designed for spinning spacecraft) are consistent with the results of the SVD analysis of STEREO data. Finally we discuss an application of the SVD method for the radio emissions with extended sources.

## 2. Determination of the Source Direction, Coherence and Apparent Size

[7] As already mentioned above, SVD is an efficient method for a wave analysis of multicomponent measurements of the magnetic field with a point source [*Santolik et al.*, 2003]. SVD can also be applied to the electric field of radio emissions by assuming  $\mathbf{E} \cdot \mathbf{k} = 0$ . Contrary to the three-axial search-coil magnetometers, effective antenna directions and lengths are different from the physical ones due to their electric coupling with the spacecraft body. Therefore one has to perform a transformation from the antenna frame into the orthonormal spacecraft system before we apply SVD (see section 4 for details). SVD provides us with a unity vector  $\boldsymbol{\kappa} = \mathbf{k}/|\mathbf{k}|$  contained in a column of the  $\mathbf{V}^T$  matrix that corresponds to the minimum of the matrix  $\mathbf{W}$  of singular values. In other words, SVD yields the direction where  $\mathbf{E}$  has the minimum of its variance. For the GP analysis of the solar radio emissions we define the angles  $\theta$  and  $\phi$ :

$$\begin{aligned} \theta &= \arctan\left(\frac{\sqrt{\kappa_1^2 + \kappa_2^2}}{\kappa_3}\right) \text{ for } \kappa_3 \geq 0, \\ \theta &= \pi - \arctan\left(\frac{\sqrt{\kappa_1^2 + \kappa_2^2}}{\kappa_3}\right) \text{ for } \kappa_3 < 0, \\ \phi &= \arctan(\kappa_2/\kappa_1), \end{aligned} \quad (11)$$

where  $\kappa_1$ ,  $\kappa_2$ , and  $\kappa_3$  are the components of the vector  $\boldsymbol{\kappa}$ . As an estimator of the wave polarization we use coherence in the polarization plane calculated by SVD. A spectral matrix is transformed into the polarization plane where we obtain coherence by comparing auto- and cross-spectra products:  $|R_{12}|/\sqrt{R_{11}R_{22}}$ , where  $R_{11}$  and  $R_{22}$  are the autopower spectra in the polarization plane, and  $R_{12}$  their cross-power spectrum. A zero coherence implies that Stokes parameters  $Q$ ,  $U$ , and  $V$  are null. We expect a very low degree of polarization in the

case of type III radio bursts. Information about the apparent source size is hidden in the  $\mathbf{W}$  matrix containing the axis lengths of the polarization ellipsoid. In an ideal case of an unpolarized radio wave with a point source, the minimum value of  $\mathbf{W}$  ( $w_1$ ) should be zero. Because of the diffusion in the solar wind, the observed radio signal is a superimposition of radio waves spread over a wide apparent source size. The ratio  $w_1/w_3$  ( $w_3$  is the maximum of  $\mathbf{W}$ ) is then nonzero and can yield information about the apparent source size. Figure 2 shows  $w_1/w_3$  as a function of the apparent source size  $\gamma$ . We have used equations (4)–(10) for modeling spectral matrices that well reflect properties of type III radio bursts at long wavelengths. We have assumed an unpolarized emission ( $Q = 0$ ,  $U = 0$ ,  $V = 0$ ). The shape of the source is considered to be uniform. For a point source ( $\gamma = 0^\circ$ ) the polarization ellipsoid changes to an ellipse contained in a single plane and the ratio of its smallest and largest axis of the ellipsoid ( $w_1/w_3$ ) is zero. On the other hand, the polarization

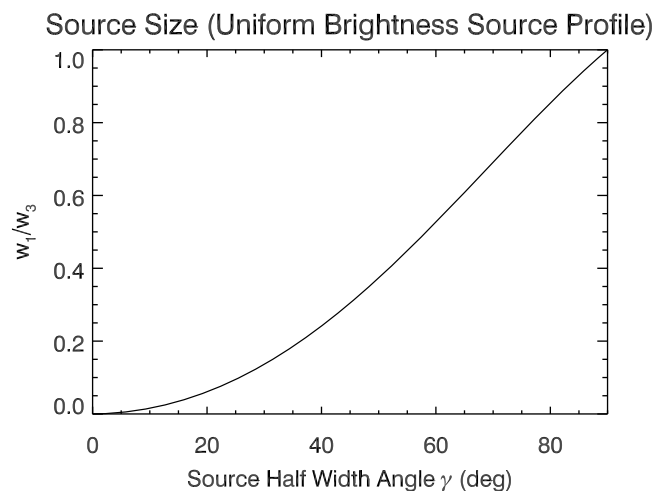


**Figure 2.** The ratio of the smallest and largest components of the diagonal matrix  $\mathbf{W}$  ( $w_1/w_3$ ) as a function of the apparent source size ( $\gamma$ ). A uniform brightness of the source and an unpolarized emission have been assumed.

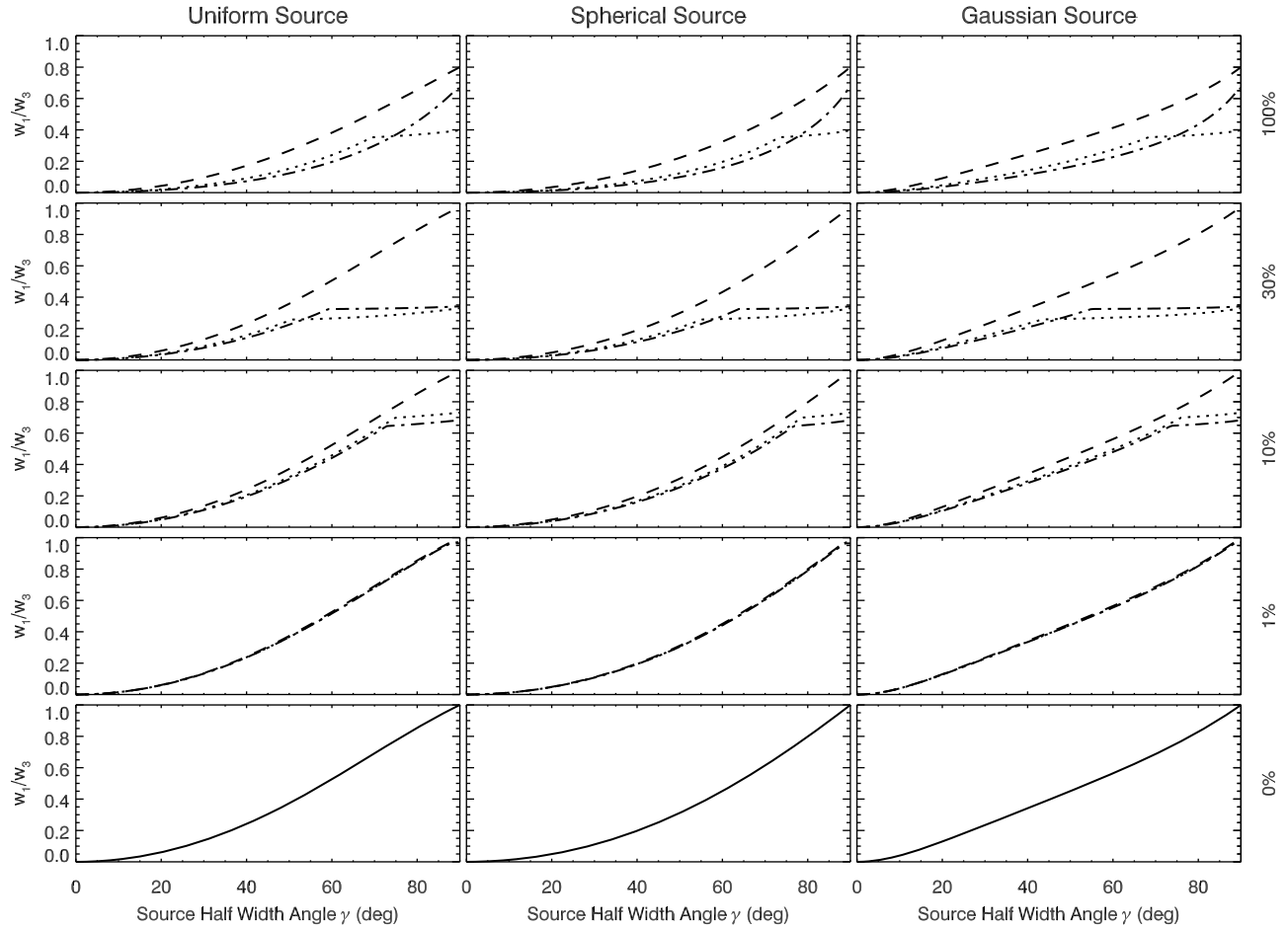


**Figure 3.** The ratio of the smallest and largest components of the diagonal matrix  $\mathbf{W}$  as a function of the apparent source size ( $\gamma$ ) with the assumption of no error of the measurements. Results for (left) uniform, (middle) spherical and (right) Gaussian brightness source profiles are shown. Degree of polarization is 100% (the first row), 30% (the second row), 10% (the third row), 1% (the fourth row) and 0% (the last row). The type of polarization has been considered to be linear (dotted lines), circular (dashed lines), or elliptical (dash-dotted lines). In case of an unpolarized emission a solid line has been used.

ellipsoid of emissions propagating from an half plane ( $\gamma = 90^\circ$ ) becomes a sphere:  $w_1/w_3 = 1$ .

### 3. Tests With Simulated Data

[8] Extensive simulations have been performed in order to validate the SVD method for estimating the apparent source size. Equations (4)–(10) have been used for modeling spectral matrices with various types and degrees of polarization computed by decreasing the normalization coefficient of the Stokes parameters (i.e., 100% polarized wave corresponds to  $\sqrt{Q^2 + U^2 + V^2} = 1$ , while 30% corresponds to  $\sqrt{Q^2 + U^2 + V^2} = 0.3$ , etc.). The SVD analysis has been applied on these simulated matrices. Figure 3 shows  $w_1/w_3$  for three shapes of the source (in columns: uniform, spherical and Gaussian) and five degrees of polarization (in rows: 100%, 30%, 10%, 1% and 0%) as a function of the apparent source size. We have investigated three possible types of polarization: the linear polarization (dashed line: 100%:  $Q = \sqrt{2}/2$ ,  $U = \sqrt{2}/2$ ,  $V = 0$ ), the right-handed

circular polarization (dotted line: 100%:  $Q = 0$ ,  $U = 0$ ,  $V = 1$ ) and the elliptical polarization (dashed dotted line: 100%:  $Q = \sqrt{3}/3$ ,  $U = \sqrt{3}/3$ ,  $V = \sqrt{3}/3$ ). A solid line in the last row refers to unpolarized emissions. When the degree of polarization is significant ( $>10\%$ ), the estimated apparent source size depends on the type of polarization. This dependence disappears if the degree of polarization is negligible. Deviations between particular source shapes are minor.

[9] The obtained empirical formulas can also be efficiently described as a 4th order polynomial regression with the independent variable as the square root of  $w_1/w_3$ :

$$\gamma(^{\circ}) = a_0 + a_1 \sqrt{\frac{w_1}{w_3}} + a_2 \left(\frac{w_1}{w_3}\right) + a_3 \left(\sqrt{\frac{w_1}{w_3}}\right)^3 + a_4 \left(\frac{w_1}{w_3}\right)^2, \quad (12)$$

where  $a_k$  are coefficients given in Table 1 for a case of an unpolarized wave that corresponds to the last row of

**Table 1.** Coefficients of a Polynomial Regression for a Case of an Unpolarized Wave for Equation (12)

$a_k$	Uniform	Spherical	Gaussian
$a_0$	0.20	-0.01	-0.42
$a_1$	75.51	90.35	60.30
$a_2$	32.70	2.86	-80.3
$a_3$	-67.62	-12.85	240.53
$a_4$	48.79	9.61	-129.53

Figure 3. Equation (12) has been used to determine  $\gamma$  in the following section.

#### 4. Analysis of a Single Type III Radio Burst Observed Simultaneously by STEREO and *Wind*

[10] STEREO are two nearly identical spacecraft dedicated to stereoscopic investigation of solar processes with varying separation angles with respect to the Sun in the ecliptic plane [Kaiser et al., 2008]. Whereas STEREO-A moves ahead of the Earth in its orbit, STEREO-B trails behind. Both spacecraft are three axis stabilized and embarking the S/Waves instrument [Bougeret et al., 2008]. The High Frequency Receiver (HFR, a part of S/Waves) provides us with GP data between 125 kHz and 1975 kHz in 38 separated bands with a 25 kHz effective bandwidth. This frequency range is well adapted to interplanetary type III radio bursts observations. HFR is a sweeping receiver with two channels from which auto- and cross-correlations are produced a posteriori. Its time resolution is about 30 s per sweep between all frequencies and antenna configurations. Three mutually orthogonal monopole antenna elements (each 6 meters in length) form the sensor part of the S/Waves instrument [Bale et al., 2008]. The effective antenna lengths and directions are different from the physical ones and can be modeled by computer simulations, estimated by rheometric measurements [Macher et al., 2007; Rucker et al., 2005; Oswald et al., 2009], or obtained by an in-flight calibration. We use the in-flight calibration using observations of the Auroral Kilometric Radiation (AKR) by STEREO-B (M. Panchenko, unpublished data, 2010). These directions are slightly different from the the w/base caps (Graz) effective antenna directions (see bottom row of Bale et al. [2008, Figure 14]). The used antenna directions can be found in the auxiliary material of this article.<sup>1</sup> As no AKR has been observed by STEREO-A during the calibration period, the effective antenna directions are assumed to be the same. The galactic background radiation has been used to determine the effective antenna lengths [Zaslavsky et al., 2011].

[11] In order to validate our GP technique, we have compared the STEREO observations with those obtained by *Wind* (located in the solar wind). Indeed this latter spacecraft which is now operating for more than 15 years can be considered to be well calibrated. The Waves instrument on-board *Wind* provides us with GP data in a frequency range from 20 up to 1040 kHz with a 3 kHz effective bandwidth [Bougeret et al., 1995]. For the GP analysis with *Wind*/Waves specific methods have been developed for spinning

spacecraft [Manning and Fainberg, 1980; Hoang et al., 1981]. These techniques provide highly accurate GP measurements using the spacecraft spin demodulation. We have considered the standard deviation of the *Wind* GP data to be  $2^\circ$  for the  $\mathbf{k}$ -vector direction as well as for the apparent source size  $\gamma$  (S. Hoang, personal communication, 2010).

[12] Figures 4 and 5 show results from STEREO-A and STEREO-B, respectively. A separation angle of STEREO-A and STEREO-B with Earth was  $4.83^\circ$  and  $2.30^\circ$  in the ecliptic plane. Both spacecraft observed an intense type III radio burst from 22:53 to 23:09 UT on May 8, 2007. It was a first intense type III radio burst recorded after both STEREO started to operate in the GP mode. To define the spacecraft positions we have used the Heliocentric Earth Ecliptic (HEE) coordinate system, which is centered on the Sun, X being the Sun-Earth line and Z pointing toward the North pole of the ecliptic. STEREO-A was located at  $[0.96, 0.08, 0.00]_{\text{HEE}}$  AU, whereas STEREO-B was at  $[1.05, -0.04, -0.01]_{\text{HEE}}$  AU. Figures 4a and 5a display the intensity of electric field fluctuations in Solar Flux Units ( $1 \text{ sfu} = 10^{-22} \text{ W}^2/\text{m}^2/\text{Hz}$ ). An intensity threshold of  $5 \times 10^3 \text{ sfu}$  has been applied to the following figures in order to suppress background and to have a good signal to noise ratio for the GP analysis. Figures 4b and 5b show the coherency in the plane of polarization calculated by the SVD. For direction finding analysis we have used Radial-Tangential-Normal (RTN) coordinates: the X axis points from the spacecraft to Sun center, the Y axis is the cross product of the solar rotational axis and X, and lies in the solar equatorial plane (toward the West limb). The observed type III radio burst propagates roughly in the ecliptic plane ( $\theta = 90^\circ$ ), as can be seen in Figures 4c and 5c containing the polar angle  $\theta$ . The azimuthal angle  $\phi$  is displayed in Figures 4d and 5d. The estimated apparent source size  $\gamma$  is contained in the Figures 4e and 5e. Figure 6 shows the same event recorded at the 925 kHz (916 kHz for *Wind*) frequency channel from both STEREO and *Wind* (located at  $[0.99, 0.00, 0.00]_{\text{HEE}}$  AU, i.e., roughly between the two STEREO). The plotted error bars for STEREO are obtained from Figures 7 and 8 with a receiver gain of 0.5 dB error (see Appendix A). The plotted error bars of the *Wind* GP data correspond to the standard deviation of  $2^\circ$ . Second and third rows contain the polar angle  $\theta$  and the azimuth angle  $\phi$ , respectively. Dashed lines represent the direction to the Sun. The last row contains the apparent source  $\gamma$  with the assumption of a uniform source brightness distribution. Dotted lines indicate values corresponding to the maximum flux at the given spacecraft. As can be seen in Figure 6, we have achieved a good agreement between STEREO and *Wind*: the estimated apparent source size  $\gamma$  is  $\sim 20^\circ$  on all three spacecraft. Table 2 contains results of the same analysis applied on intense type III radio bursts observed in May 2007, when separation angles between all spacecraft were below  $12^\circ$ .

#### 5. Discussion and Conclusion

[13] The two STEREO spacecraft provide a great opportunity for stereoscopic observations of solar radio emissions at long wavelengths. The *Wind* spacecraft, located roughly between them, is ideal for complementary measurements. The S/Waves instruments on-board STEREO provide GP

<sup>1</sup>Auxiliary material data sets are available at <ftp://ftp.agu.org/apend/ja/2011ja017333>. Other auxiliary material files are in the HTML. doi:10.1029/2011JA017333.

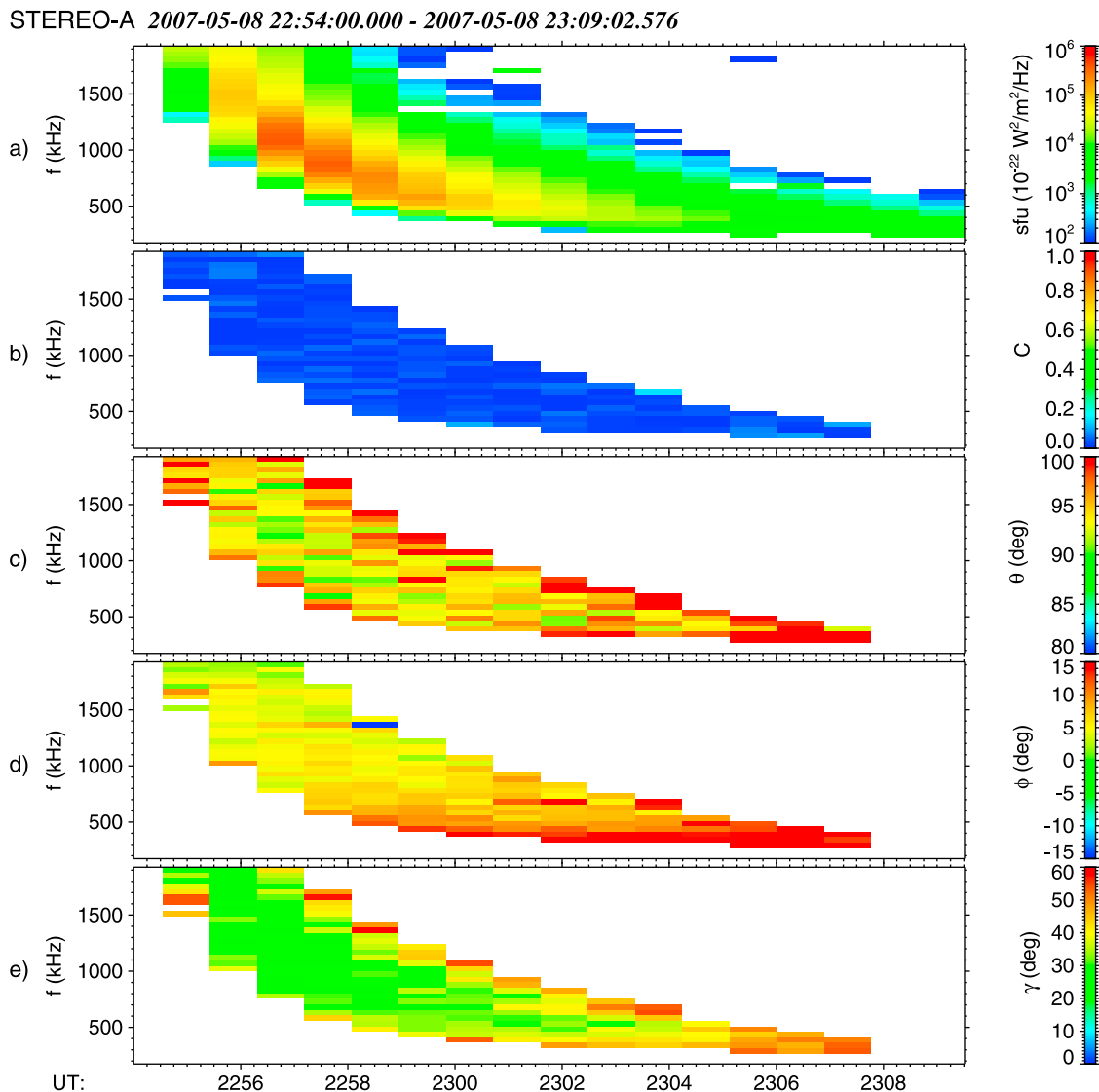


**Figure 4.** From 22:53 to 23:09 UT on 8 May 2007: (a) the electric field spectral density, (b) the coherence, (c) the polar angle  $\theta$ , (d) the azimuthal angle  $\phi$ , and (e) the apparent source size  $\gamma$  for STEREO-A.

data that allow to retrieve the  $\mathbf{k}$ -vector direction and polarization properties. An analysis of three type III radio bursts recorded by both STEREO and *Wind*, and using different methods than in this paper, has been done by *Reiner et al.* [2009]. Preliminary results of an application of SVD to measurements of emissions with very extended sources has been recently published by *Krupar et al.* [2010]. Results of a triangulation of radio sources can be also compared with the coronagraph images [*Howard et al.*, 2008; *Martínez Oliveros et al.*, 2012]. A combination of a suitable separation angle between two spacecraft (a triangulation works best for  $40^\circ$ – $60^\circ$ ) and the increased solar activity (when more phenomena may be observed) will be reached in 2014. GP capabilities of STEREO may improve our understanding of generation mechanisms of type II and type III radio bursts.

[14] The main result of the paper is the GP inversion using SVD of a signal measured on non-orthogonal antennas with a focus on investigating type III radio bursts at long

wavelengths, which have very extended sources and a low degree of polarization. This is the first time that such a technique is applied for a three axis stabilized spacecraft. In section 2 we have obtained an empirical relation between the decomposed spectral matrices, that contains lengths of the polarization ellipsis, and the apparent source sizes for unpolarized emissions with a uniform source shape (Figure 2). For a point source ( $\gamma = 0^\circ$ ) the polarization ellipsoid degenerates to an ellipse ( $w_1/w_3 = 0$ ), whereas for a very extended source ( $\gamma = 90^\circ$ ) it becomes a sphere ( $w_1/w_3 = 1$ ).

[15] An extensive study of various types and degrees of polarization has been performed in section 3. A uniform, spherical and Gaussian source profiles have been considered (Figure 3). We have shown that the empirical relations for these particular shapes of source brightness are similar. If the degree of polarization is below 10% then the differences between the various types of polarization vanish. Otherwise one has to identify the type of polarization in order to apply the appropriate empirical relation.

STEREO-B 2007-05-08 22:54:00.000 - 2007-05-08 23:08:43.592

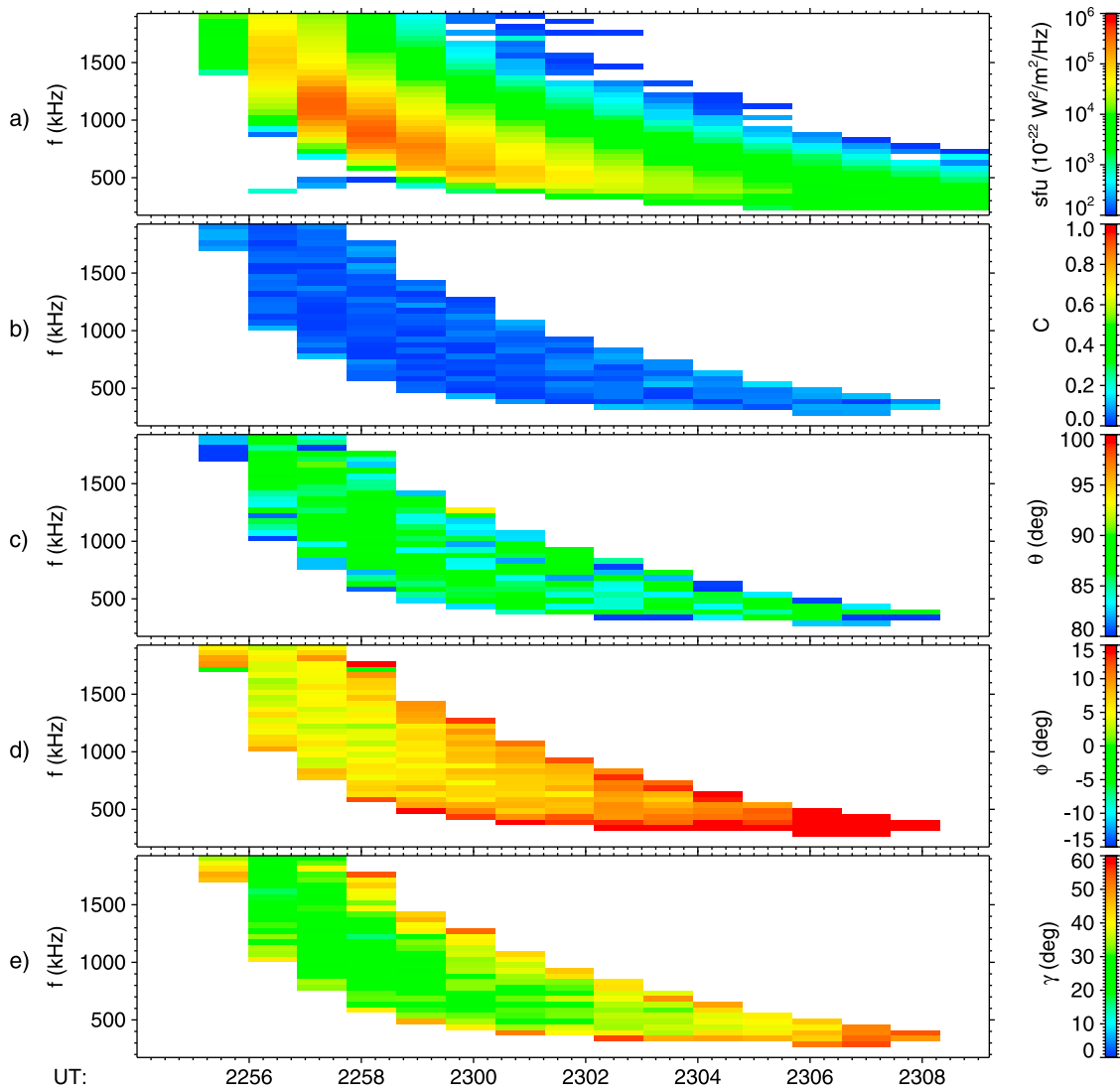


**Figure 5.** From 22:53 to 23:09 UT on 8 May 2007: (a) the electric field spectral density, (b) the coherence, (c) the polar angle  $\theta$ , (d) the azimuthal angle  $\phi$ , and (e) the apparent source size  $\gamma$  for STEREO-B.

[16] As an example we present an observation of a type III radio burst obtained simultaneously by the two STEREO and *Wind* spacecraft during small separation distances. Figures 4b and 5b which display the coherency show that the observed type III radio burst has almost no polarized part, as expected at these wavelengths. The type III radio burst propagates roughly in the ecliptic plane ( $\theta = 90^\circ$ , see Figures 4c and 5c) and eastward from the Sun ( $\phi > 0^\circ$ ) accordingly to the Parker spiral geometry (see Figures 4d and 5d). For higher frequencies the radio source is located roughly in the Sun direction, whereas the source moves eastward as the frequency decreases (see Figures 4d and 5d). Scattering effects due to density fluctuations of the solar wind are more significant for lower frequencies. The apparent source sizes vary between  $20^\circ$  and  $40^\circ$  on both spacecraft (see Figures 4e and 5e) with a slight increase of gamma for lower frequencies. The time and frequency center of the burst has smaller  $\gamma$  than its surrounding.

[17] Figure 6 shows results for the same event from the 925 kHz (916 kHz for *Wind*) frequency channel. Errors induced by the uncertainty on the HFR receiver gain have been taken into account (see Appendix A). We can distinguish an intense peak at 22:58 (the first row of Figure 6). The measured fluxes are about the same for both STEREO. We obtain a better agreement in  $\mathbf{k}$ -vector directions at both frequency channels between *Wind* and STEREO-B, within their respective error bars, than between STEREO-A and *Wind*. The apparent source size is shown in the last row. Although a Gaussian source shape would probably better reflect real observations, the parameter  $\gamma$  from *Wind* has been obtained from previously processed data considering a uniform source shape (S. Hoang, personal communication, 2010). During the maximum of intensity the source size calculated by SVD on STEREO is about the same ( $\gamma_{925} \sim 20^\circ$ ) as on *Wind* which is using a different method dedicated for spinning spacecraft. The best agreement

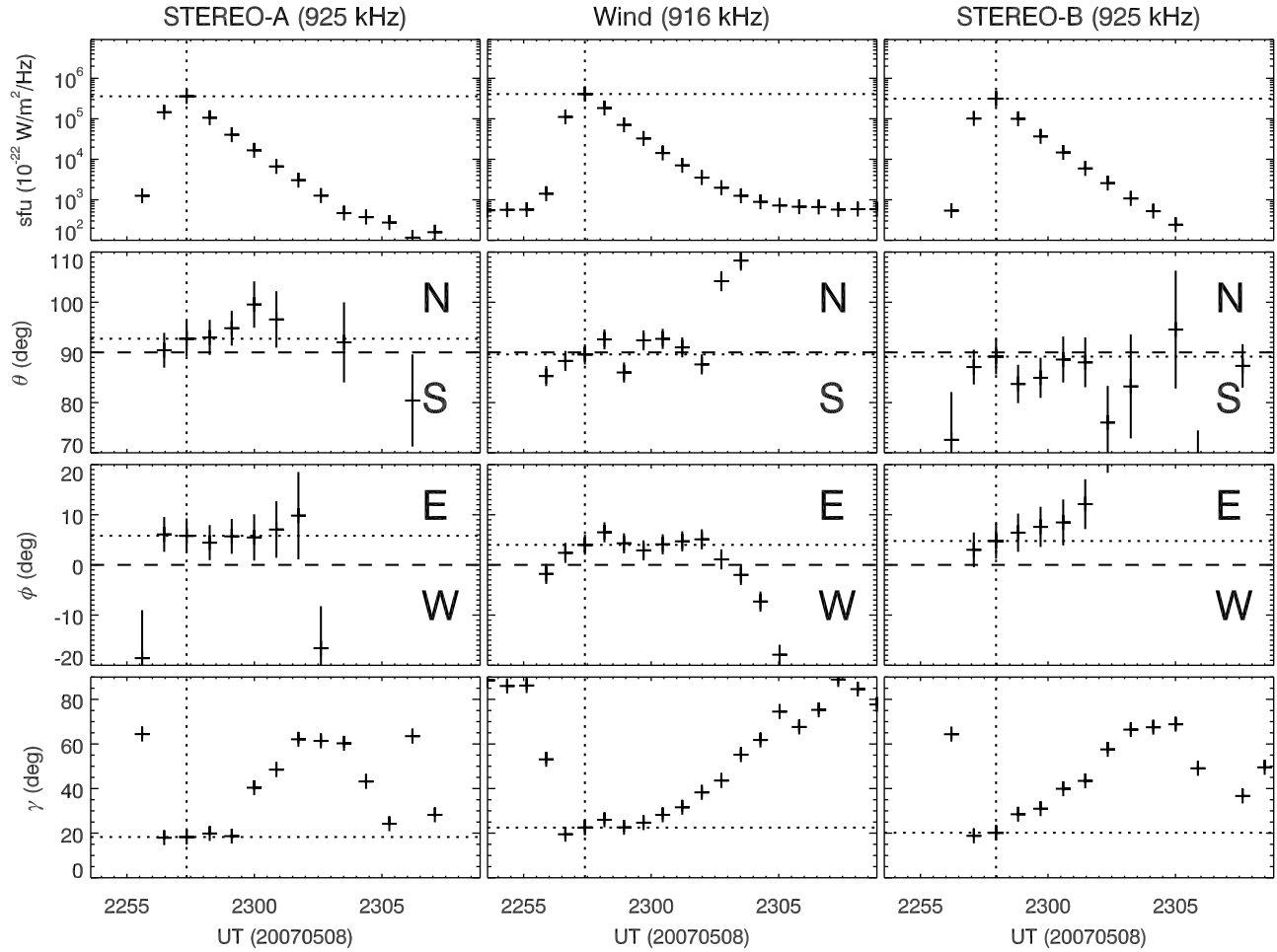


**Figure 6.** From 22:53 to 23:09 UT on 8 May 2007: the electric field spectral density, the polar angle  $\theta$ , the azimuthal angle  $\phi$  (in the RTN coordinate system) and the apparent source size  $\gamma$  for STEREO-A (925 kHz), Wind (916 kHz) and STEREO-B (925 kHz). Dashed lines represent the direction to the Sun. Dotted lines indicate values corresponding to the maximum flux at the given spacecraft.

**Table 2.** Apparent Source Sizes  $\gamma$  Calculated for Six Intense Type III Radio Bursts From May 2007 During Peak Fluxes<sup>a</sup>

Time <sub>STEREO - A</sub>	$f_{\text{STEREO}}$ (kHz)	$f_{\text{Wind}}$ (kHz)	$\gamma_{\text{STEREO - A}}$ (deg)	$\gamma_{\text{Wind}}$ (deg)	$\gamma_{\text{STEREO - B}}$ (deg)
2007-05-08T23:07:47.459	225	224	35.67	41.30	49.06
2007-05-08T22:58:10.809	625	624	17.28	24.30	22.68
2007-05-08T22:57:20.523	925	916	18.28	22.50	20.20
2007-05-15T15:46:29.454	225	224	52.12	39.10	57.18
2007-05-15T15:39:30.276	625	624	21.16	25.30	11.75
2007-05-15T15:37:49.166	925	916	24.33	23.90	24.41
2007-05-19T13:11:22.259	225	224	35.07	33.90	25.13
2007-05-19T12:57:26.010	625	624	24.69	24.90	14.10
2007-05-19T12:56:37.721	925	916	17.09	23.80	23.47
2007-05-22T14:37:42.407	225	224	42.58	49.00	43.09
2007-05-22T14:31:38.545	625	624	24.74	24.50	16.71
2007-05-22T14:30:47.751	925	916	19.57	23.70	14.51
2007-05-23T07:35:03.647	225	224	44.91	34.90	37.43
2007-05-23T07:23:39.854	625	624	23.54	23.70	22.73
2007-05-23T07:22:51.070	925	916	21.03	19.90	11.78
2007-05-30T20:44:02.645	225	224	45.94	45.40	50.13
2007-05-30T20:36:13.137	625	624	21.51	28.20	17.73
2007-05-30T20:34:30.031	925	916	19.96	24.00	11.67

<sup>a</sup>The first column corresponds to peak fluxes observed by STEREO-A. A VOTable formatted version is available in the auxiliary material (see Data Set S1).

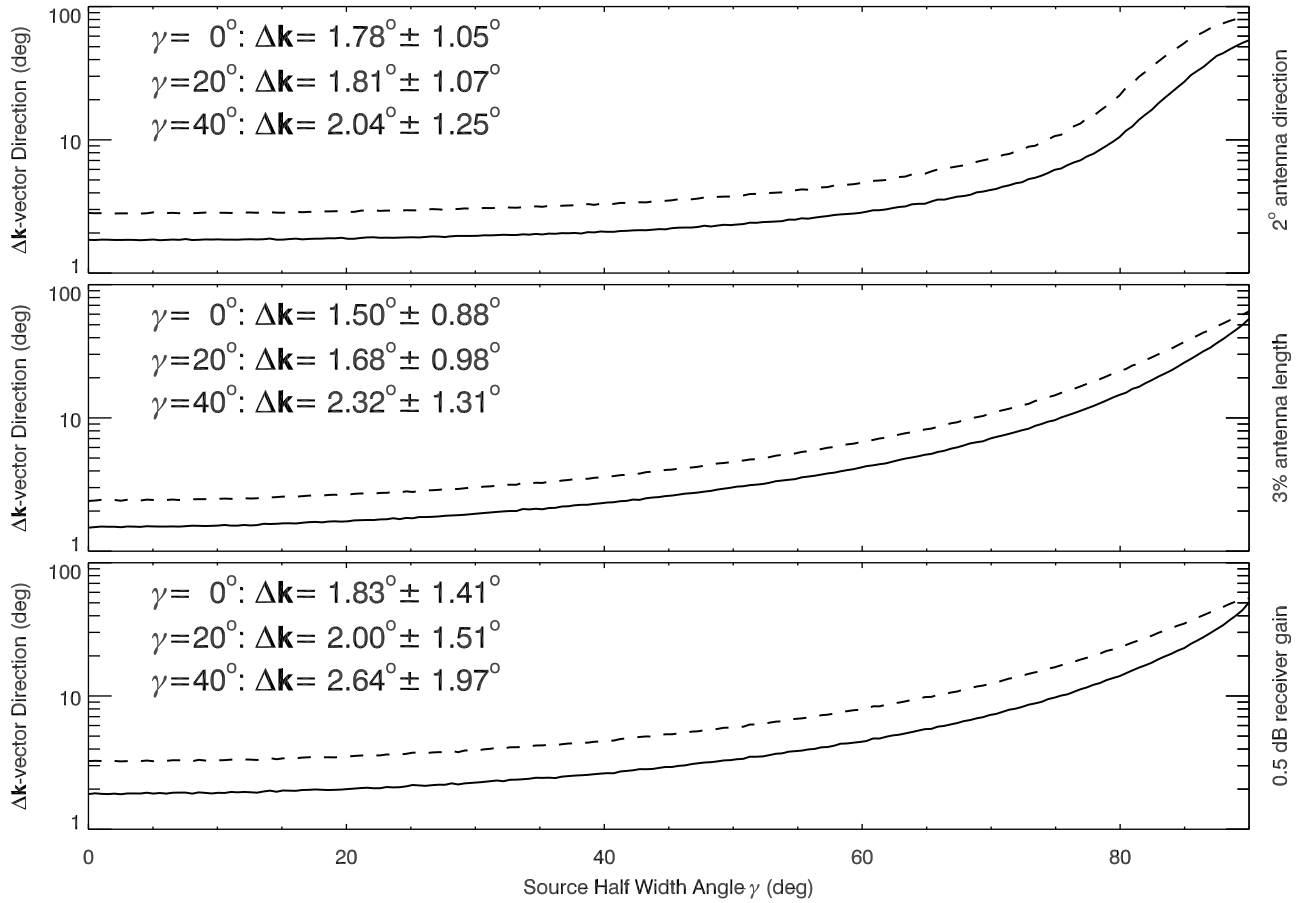


**Figure 7.** An average angle difference between an input  $\mathbf{k}$ -vector direction and the obtained one by SVD as a function of the apparent source size  $\gamma$  is represented by a solid line, a dashed line is the average plus its standard deviation. (top) An inaccuracy of effective antenna directions of  $2^\circ$ ; (middle) an inaccuracy of effective antenna lengths of 3%; (bottom) an uncertainty on the receiver gain of 0.5 dB.

between STEREO and Wind is achieved during a peak flux since the polarization is nearly zero (an initial assumption of the empirical relation in this paper) and the signal-to-noise ratio is relatively high. It confirms the validity of our empirical relation for estimating the apparent source size. Other case studies of joint STEREO and *Wind* observations with small separation distances give similar results (see Table 2). We have obtained a better agreement for the first three events. One should note here that the effective bandwidth of both STEREO is 25 kHz whereas *Wind* has 3 kHz only. It indicates that the SVD method we use and the empirically derived relations can be used for type III radio bursts GP observations. This method can either be used for statistical studies where one needs a robust and fast data processing or for the estimation of initial values that can be used for a more complete GP method using a standard non-linear  $\chi^2$  fitting.

[18] Our study leads us to the following conclusions: 1. We have demonstrated that the SVD allows to directly retrieve the  $\mathbf{k}$ -vector direction from electric field measurements in the case of type III radio bursts. 2. We have found the empirical relation between the decomposed spectral matrices and the apparent source sizes for unpolarized radio emissions with a special focus on type III radio bursts observed by STEREO; 3. Other possible degrees and types

of polarization have been also studied with our method and we have shown that below 10% of polarized part it is not necessary to distinguish the type of polarization; 4. Finally one should note that such GP method will also be implemented on the Radio Plasma Waves instrument [Boudjada *et al.*, 2005] on-board the Solar Orbiter spacecraft which, as STEREO, will be three-axis stabilized.

#### Appendix A: Error Analysis on the Estimation of the Wave Vector Direction and Apparent Size

[19] We have investigated the influence of several possible errors that can affect the current GP inversion applied to Type III bursts. We have performed an error analysis taking into account inaccuracies of the effective antenna directions ( $2^\circ$ ) and lengths (3%) and an uncertainty on the receiver gain (0.5 dB). The amplitudes of these errors correspond to values estimated from properties of the S/Waves HFR receiver which has been used in section 4 for a demonstration of our analysis. We have simulated antenna directions with normal distributions of absolute deviations centered on the nominal direction with sigma of  $2^\circ$ , and uniform distributions of azimuth. We have also applied the Gaussian noise with a standard deviation of 3% on antenna lengths. As another source of an error an uncertainty on the receiver gain

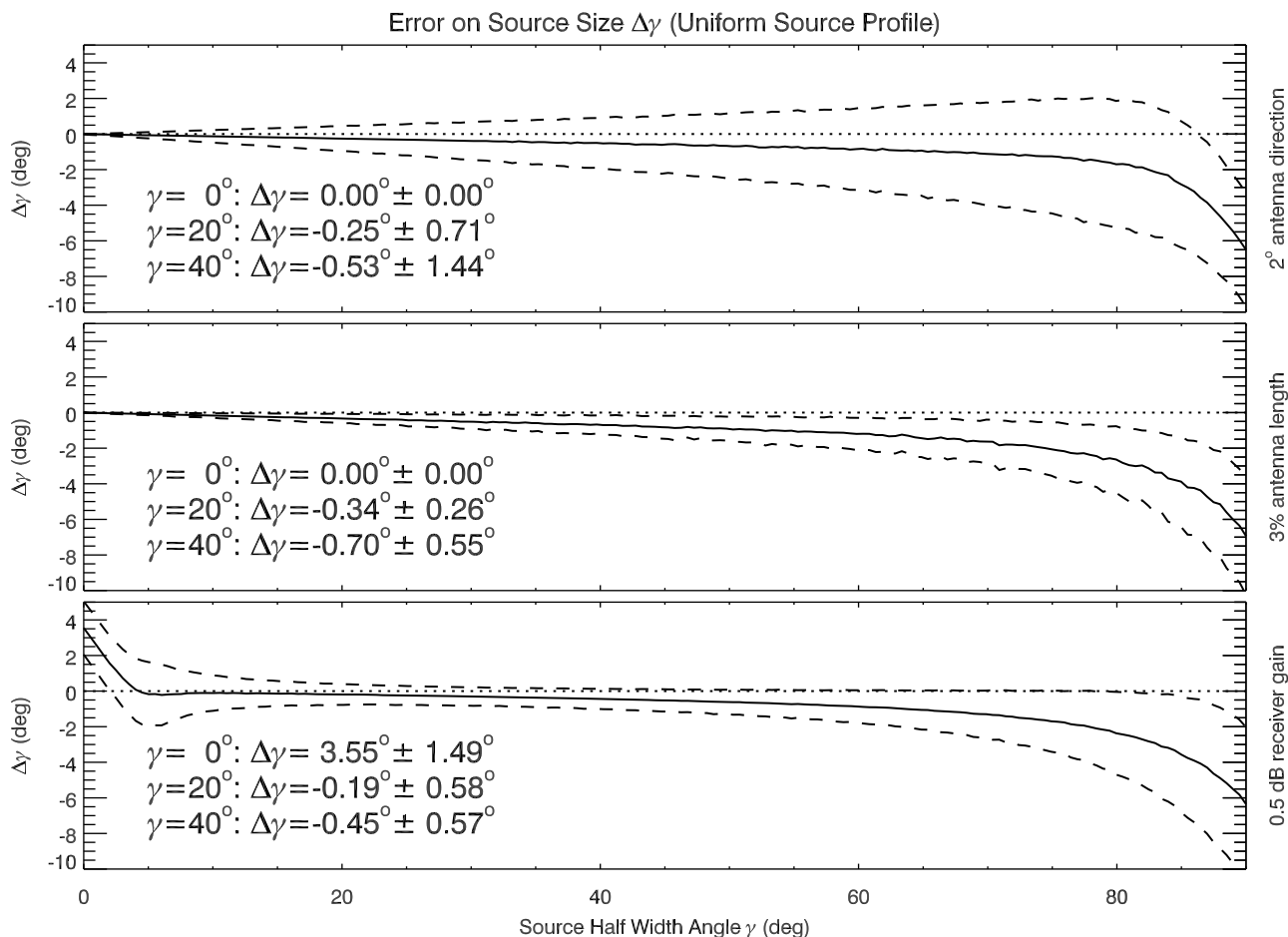


**Figure 8.** An average angle difference between an input  $\gamma$  and the obtained one by SVD as a function of the apparent source size  $\gamma$  is represented by a solid line, a dashed line is the average plus/minus its standard deviation. First row: an inaccuracy of effective antenna directions of 2°; Second row: an inaccuracy of effective antenna lengths of 3%; Third row: an uncertainty on the receiver gain of 0.5 dB.

has been considered when we have applied the Gaussian noise on the final auto/cross-correlation products (normal distributions of the uncertainties in dB centered at 0 dB). Figure 7 shows an angle difference between an input  $\mathbf{k}$ -vector direction and an output one obtained by SVD as a function of the apparent source size with an assumption of the errors mentioned above. As  $\gamma$  is larger the uncertainty of estimation of the  $\mathbf{k}$ -vector direction increases, as it has been expected. Figure 8 contains an angle difference between an input  $\gamma$  and an output one obtained by SVD (the empirical relation) as a function of the apparent source size. For small sources ( $\gamma < 5^\circ$ ) the empirical relation overestimates the source size. On the other hand, the empirical relation underestimates the source size for large sources ( $\gamma > 60^\circ$ ). Regarding Figures 7 and 8 we conclude that the largest influence that can affect our measurements is an uncertainty on the receiver gain. Therefore it has been considered as a main source of errors in the paper.

[20] **Acknowledgments.** The authors thank Pierre-Luc Astier and Quynh Nhu Nguyen (from LESIA) for providing the S/Waves data and useful engineering insights on the receiver functions. The present work was supported by a scholarship from the French government, grants KONTAKT ME9107, GACR P205102279, and GACR P209122394. The French sub-systems of the S/Waves experiment have been built by

LESIA with the support from both CNES and CNRS. M. Panchenko acknowledges the Austrian Fond zur Foerderung der wissenschaftlichen Forschung (FWF project P20680-N16).

[21] Philippa Browning thanks the reviewers for their assistance in evaluating this paper.

## References

- Bale, S. D., et al. (2008), The electric antennas for the STEREO/WAVES experiment, *Space Sci. Rev.*, 136, 529–547, doi:10.1007/s11214-007-9251-x.
- Bonnin, X., S. Hoang, and M. Maksimovic (2008), The directivity of solar type III bursts at hectometer and kilometer wavelengths: Wind-Ulysses observations, *Astron. Astrophys.*, 489, 419–427, doi:10.1051/0004-6361:200809777.
- Boudjada, M. Y., W. Macher, H. O. Rucker, and G. Fischer (2005), Solar orbiter: Physical aspects towards a better knowledge of the solar corona, *Adv. Space Res.*, 36, 1439–1443, doi:10.1016/j.asr.2005.05.118.
- Bougeret, J.-L., et al. (1995), Waves: The radio and plasma wave investigation on the Wind spacecraft, *Space Sci. Rev.*, 71, 231–263, doi:10.1007/BF00751331.
- Bougeret, J. L., et al. (2008), S/WAVES: The radio and plasma wave investigation on the STEREO mission, *Space Sci. Rev.*, 136, 487–528, doi:10.1007/s11214-007-9298-8.
- Cairns, I. H., and P. A. Robinson (1995), Ion acoustic wave frequencies and onset times during type III solar radio bursts, *Astrophys. J.*, 453, 959–972, doi:10.1086/176456.
- Cecconi, B. (2007), Influence of an extended source on goniopolarimetry (or direction finding) with Cassini and Solar Terrestrial Relations

- Observatory radio receivers, *Radio Sci.*, 42, RS2003, doi:10.1029/2006RS003458.
- Cecconi, B., et al. (2008), STEREO/waves goniopolarimetry, *Space Sci. Rev.*, 136, 549–563, doi:10.1007/s11214-007-9255-6.
- Dulk, G. A. (2000), Type III solar radio bursts at long wavelengths, in *Radio Astronomy at Long Wavelengths*, *Geophys. Monogr. Ser.*, vol. 119, edited by R. G. Stone et al., pp. 115–122, AGU, Washington D. C.
- Ginzburg, V. L., and V. V. Zhelezniakov (1958), On the possible mechanisms of sporadic solar radio emission (radiation in an isotropic plasma), *Sov. Astron., Engl. Transl.*, 2, 653–664.
- Gurnett, D. A., M. M. Baumbach, and H. Rosenbauer (1978), Stereoscopic direction finding analysis of a type III solar radio burst: Evidence for emission at  $2f_p^-$ , *J. Geophys. Res.*, 83, 616–622, doi:10.1029/JA083iA02p00616.
- Hoang, S., J. L. Steinberg, R. G. Stone, R. H. Zwickl, and J. Fainberg (1981), The  $2f_p^-$  circumterrestrial radio radiation as seen from ISEE 3, *J. Geophys. Res.*, 86, 4531–4536, doi:10.1029/JA086iA06p04531.
- Howard, R. A., et al. (2008), Sun Earth Connection Coronal and Heliospheric Investigation (SECCHI), *Space Sci. Rev.*, 136, 67–115, doi:10.1007/s11214-008-9341-4.
- Kaiser, M. L., T. A. Kucera, J. M. Davila, O. C. St. Cyr, M. Guhathakurta, and E. Christian (2008), The STEREO mission: An introduction, *Space Sci. Rev.*, 136, 5–16, doi:10.1007/s11214-007-9277-0.
- Kraus, J. D. (1966), *Radio Astronomy*, McGraw-Hill, New York.
- Krupar, V., M. Maksimovic, O. Santolik, B. Cecconi, Q. N. Nguyen, S. Hoang, and K. Goetz (2010), The apparent source size of type III radio bursts: Preliminary results by the STEREO/WAVES instruments, *AIP Conf. Proc.*, 1216, 284–287, doi:10.1063/1.3395856.
- Ladreitner, H. P., P. Zarka, A. Lecacheux, W. Macher, H. O. Rucker, R. Manning, D. A. Gurnett, and W. S. Kurth (1995), Analysis of electromagnetic wave direction finding performed by spaceborne antennas using singular-value decomposition techniques, *Radio Sci.*, 30, 1699–1712, doi:10.1029/95RS02479.
- Lecacheux, A. (1978), Direction finding of a radiosource of unknown polarization with short electric antennas on a spacecraft, *Astron. Astrophys.*, 70, 701–706.
- Macher, W., T. H. Oswald, G. Fischer, and H. O. Rucker (2007), Rheometry of multi-port spaceborne antennas including mutual antenna capacitances and application to STEREO/WAVES, *Meas. Sci. Technol.*, 18, 3731–3742, doi:10.1088/0957-0233/18/12/008.
- Manning, R., and J. Fainberg (1980), A new method of measuring radio source parameters of a partially polarized distributed source from spacecraft observations, *Space Sci. Instrum.*, 5, 161–181.
- Martínez Oliveros, J. C., C. L. Raftery, H. M. Bain, Y. Liu, V. Krupar, S. Bale, and S. Krucker (2012), The 2010 August 1 type II burst: A CME-CME interaction and its radio and white-light manifestations, *Astrophys. J.*, 748, 66, doi:10.1088/0004-637X/748/1/66.
- Oswald, T. H., W. Macher, H. O. Rucker, G. Fischer, U. Taubenschuss, J. L. Bougeret, A. Lecacheux, M. L. Kaiser, and K. Goetz (2009), Various methods of calibration of the STEREO/WAVES antennas, *Adv. Space Res.*, 43, 355–364, doi:10.1016/j.asr.2008.07.017.
- Reiner, M. J., K. Goetz, J. Fainberg, M. L. Kaiser, M. Maksimovic, B. Cecconi, S. Hoang, S. D. Bale, and J.-L. Bougeret (2009), Multipoint observations of solar type III radio bursts from STEREO and Wind, *Sol. Phys.*, 259, 255–276, doi:10.1007/s11207-009-9404-z.
- Rucker, H. O., W. Macher, G. Fischer, T. Oswald, J. L. Bougeret, M. L. Kaiser, and K. Goetz (2005), Analysis of spacecraft antenna systems: Implications for STEREO/WAVES, *Adv. Space Res.*, 36, 1530–1533, doi:10.1016/j.asr.2005.07.060.
- Santolik, O., M. Parrot, and F. Lefeuvre (2003), Singular value decomposition methods for wave propagation analysis, *Radio Sci.*, 38(1), 1010, doi:10.1029/2000RS002523.
- Steinberg, J. L., S. Hoang, A. Lecacheux, M. G. Aubier, and G. A. Dulk (1984), Type III radio bursts in the interplanetary medium: The role of propagation, *Astron. Astrophys.*, 140, 39–48.
- Steinberg, J. L., S. Hoang, and G. A. Dulk (1985), Evidence of scattering effects on the sizes of interplanetary type III radio bursts, *Astron. Astrophys.*, 150, 205–216.
- Weber, R. R. (1978), Low frequency spectra of type III solar radio bursts, *Sol. Phys.*, 59, 377–385, doi:10.1007/BF00951843.
- Wild, J. P. (1950), Observations of the spectrum of high-intensity solar radiation at metre wavelengths: III. Isolated bursts, *Aust. J. Sci. Res., Ser. A*, 3, 541–557.
- Zaslavsky, A., N. Meyer-Vernet, S. Hoang, M. Maksimovic, and S. D. Bale (2011), On the antenna calibration of space radio instruments using the galactic background: General formulas and application to STEREO/WAVES, *Radio Sci.*, 46, RS2008, doi:10.1029/2010RS004464.